System Level Simulation And Fabrication Of SOI-MEMS Differential Capacitive Accelerometer

Veena.S[1,*], H.L Suresh[2], Newton Rai[3], Veerapandi N[4], and Veda Sandeep Nagaraj[5]

[1] Department of Electrical and Electronics Engineering, Nitte Meenakshi Institute of Technology, Bangalore
[2] Department of Electrical and Electronics Engineering, Sir.M Visvesvaraya Institute of Technology, Bangalore
[3] Mechanical Department, University of Colorado Boulder
[4] Centre for Nano Science and Engineering(CeNSE), Indian Institute of Science(IISc), Bangalore
[5] Tyndall National Institute, University College Cork, Ireland
[*] Corresponding author. E-mail: veena.murthy80@gmail.com

Received: Dec. 13, 2022; Accepted: Jun. 21, 2023

This study primarily covers the design and development of an MEMS based accelerometer. Frequency, displacement sensitivity, and capacitance are the subject of analytical modelling; the corresponding values are found to be 7.41kHz, $4.5096{*}10^{-9}$ m/g, and 0.289pF respectively. COMSOL Multiphysics is used to design the structure of accelerometer and the MATLAB simulator tool is used to analyse the accelerometer. In order to obtain precise results, simulations are done and theoretical calculations are compared. Silicon-on-Insulator Multi-User MEMS Processes (SOIMUMPS) technology is employed to fabricate the accelerometer structure at MEMSCAP foundry, United State. The characterization of the fabricated device is done at CENSE, IISc, Bangalore. The capacitance values on either side of the device obtained from the test results are 0.36pF and 0.85pF when 5 V is applied to the electrodes. The proposed accelerometer is employed in the actuating parts of the sensor due to its properties like linearity and low sensitivity.

Keywords: MEMs Capacitive Accelerometer, COMSOL, SOI MUMPS, Fabrication, Characterisation, Sensitivity.
© The Author('s). This is an open-access article distributed under the terms of the Creative Commons Attribution License (CC BY 4.0), which permits unrestricted use, distribution, and reproduction in any medium, provided the original author and source are cited.

http://dx.doi.org/10.6180/jase.202403_27(3).0012

1. Introduction

MEMS inertial sensors are very commonly used in number of ranges of applications which require motion sensing such as, in automobiles for air bag deployment, aerospace applications for navigation, smart phones etc [1]. Capacitive technology is favoured over other existing mechanisms such as piezoresistive and piezoelectric for sensing applications because of its benefits, including good linearity, low power dissipation, less sensitive to temperature and noise, and simplicity of readout circuitry [2]. Silicon on Insulator (SOI) based MEMS accelerometer which ensures low power consumption, high resolution, high performance and miniaturization is the need of the day. High quality etch profile can be attained using Deep Reactive Ion Etching (DRIE), the gap between sensing fingers can be realised using DRIE process where larger capacitive sensitivity can be achieved by increasing the number of the sensing fingers and its overlap area [3]. Due to the efficient isolation of the active and bulk layers, SOI wafers have improved mechanical and electrical performance, resilience, and parasitics. Furthermore, they work well with the DRIE process. Because DRIE-SOI process has greater performance and good control over the high-aspect-ratio (HAR) structure geometry, it is chosen over other techniques, such as surface micromachining, LIGA process, and wet micromachining [4]. Hence the accelerometer structure presented in this paper is SOI based and fabricated using DRIE technique. SOIMUMPS process is used for the fabrication of the proposed device at MEMSCAP foundry, and it uses Bulk Micromachining

and DRIE process. It is essential to take the residual stress into account while running simulations and mathematically modelling the device when the SOI wafer is wafer bonded.

However, the impact of residual stress is not considered in this work. A MEMS accelerometer contains a seismic mass which is supported by beams. While modeling mass is typically added to a dashpot, which provides the necessary damping effects. The spring and dashpot are each linked to the frame in turn. An accelerometer at rest on the surface of the earth will measure the acceleration caused by gravity (g = 9.81 m/s^2), whereas an accelerometer in free fall will measure zero [5]. To analyse the characteristics of the device, the mathematical analysis was conducted in accordance with damping. The capacitive based MEMS accelerometers evaluate the capacitance fluctuation between an anchored conductive electrode and a proof mass that is separated by a very narrow distance. Here, the accelerometer's sensitivity is a measurement of displacement with reference to acceleration. COMSOL multiphysics tool is used to simulate the proposed structure. The organization of the paper is as follows: section 2 and 3 showcases the structure and design of the accelerometer. The simulation results and the testing of capacitive type, single axis in-plane SOI-MEMS accelerometer fabricated in SOIMUMPs is discussed in 4 and 5 sections respectively. Results and discussion in section 6 and the work is concluded in section 7.

2. Device structure

The capacitive accelerometer is composed of 2 parts, movable and fixed. The movable part comprises of two proof masses of area $200 \times 400\mu$m and are symmetrically suspended by folded beam to the central anchor on one side and has comb fingers (13 numbers) of dimension 250×10 μm on the other side. These comb fingers are interleaved between the anchored outer fingers (14 numbers) of dimension $250 \times 10\mu$m of the fixed electrodes $(100 \times 400\mu\text{m})$ as shown in the Fig. 1. The proposed accelerometer is designed in a total area of $1400 \times 400\mu$m. The gap between the driving and the sensing fingers is 5μm and the overlap area between the two is 245μm as shown in the Fig. 2.

Some of the common characteristics that determine the performance of the accelerometers are capacitance sensitivity, electrostatic force, electrostatic spring constant, maximum operation range, frequency response, resonant frequency, resolution, full-scale nonlinearity, offset, off-axis sensitivity, and shock endurance [6]. Some of these characteristics will be important in terms of design considerations depending on the type of application.

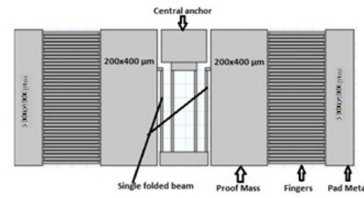

Fig. 1. Proposed accelerometer structure.

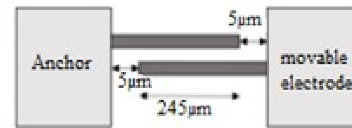

Fig. 2. Positioning of the combs in the accelerometer.

Likewise, the movable fingers interleaved with the fixed fingers establish the differential capacitance C1 and C2 on either side of the proof mass as shown in Fig. 3a and Fig. 3b.

The amount of force applied to the proof mass and its direction can be found by measuring the differential capacitance on either side of the accelerometer structure. This differential, and the voltage associated with it can be calculated from the following Eq. (1) [7]

$$\mathrm{V_S} = \mathrm{V_{out}} = \frac{(C_1 - C_2)}{(C_1 + C_2)} V_m \tag{1}$$

Where Vm is the applied voltage and Vs is the output voltage.

3. Electromechanical design aspects of the proposed accelerometer

The analytical calculations of the proposed accelerometer structure is presented in Table 1 [7].

Where E = Young's modulus of elasticity (silicon) = $170 * 10^9$ $\mathrm{N/m^2}$, t = thickness of beam = 25μm, W = Width of beam = 10μm and L = length of beam = 245μm. Pa is Ambient pressure $(1.01 \times 10^{-5}$ Pa$)$, σ = compression ratio of air, u = coefficient of dynamic viscosity (1.85×10^{-5}).

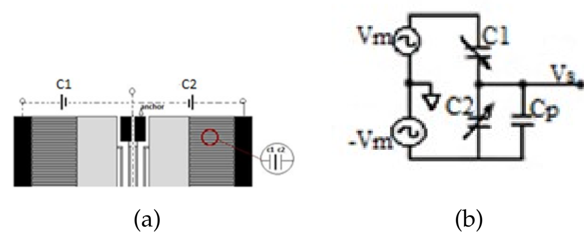

(a) (b)

Fig. 3. (a)Accelerometer lateral view & (b) Accelerometer working principle

Table 1. Analytical calculations of the accelerometer.

Natural frequency	$f_n = \frac{1}{2\pi}\sqrt{\frac{k}{m}}$	$f_n = 7.41$kHz
	Stiffness of beam $= K = \frac{EtW^3}{4L^3}$	$K = 31$ N/m
	Total mass, m=mass of (proof mass+ Sensing fingers)	$m = 1.42651*10^{-9}$Kg
Damping Ratio	$\zeta = \frac{b}{2m\omega_n}$	$\zeta = 0.0549$
	Damping Co efficient,	$b = 7.304 * 10^{-6}$Ns/m
	$W_n = 2\pi f$	$W_n = 14820\pi$Hz
	$\sigma = \frac{12uw^2 w_n}{p_a g^2}$	$\sigma = 0.19576$
	$B = L/W$	$B = 24.5$
Static capacitance	$C_0 = \frac{EN_f l_f t}{d_o}$	$C_0 = 0.28199$pF
Displacement sensitivity	$S_d = x = \frac{m}{K} * a$	$S_d = 4.5096*10^{-9}$ m/g

comb finger length $(l_f) = 245\mu$m, total movable fingers $(N_f) = 13$, finger thickness $(t) = 25\mu$m, distance between two adjacent fingers $(d_o) = 5\mu$m.

The nature of the system response is directly influenced by the value of the damping ratio. According to the data in Table 1 , the suggested accelerometer has a damping ratio of less than 1 , making it an under damped system.

4. Simulation and results

Simulation studies are performed to understand the effect of frequency, acceleration, and stress on the displacement of the proof mass. COMSOL Multiphysics tool is used for performing simulation study on the proposed accelerometer [8].

(A) Frequency simulation: The structure is simulated to examine the deformation of the accelerometer at resonant frequency. The simulated frequency obtained using single crystal silicon as the base material is 7.074 kHz, as illustrated in Fig. 4.

(B) Displacement simulation: In Fig. 5, we see the proof mass being displaced in response to an applied force on the accelerometer. The overall shift is estimated to be 6.03×10^{-9} m.

(C) Stress simulation: Stationary analysis in COMSOL Multiphysics is performed to learn the device's stress tolerance at 1 g. As can be observed in Fig. 6, the upper half of the device may fail with a stress of over $6.84\text{X}10^3$ N/m^2.

(D) Capacitance Simulation: The proposed structure's capacitance is determined by an electrostatic study performed in the COMSOL software. Fig. 7 displays the accelerometer's static capacitance and is found to be 0.275pF.

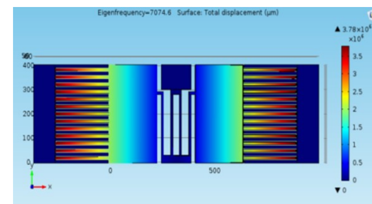

Fig. 4. Frequency simulation of the structure.

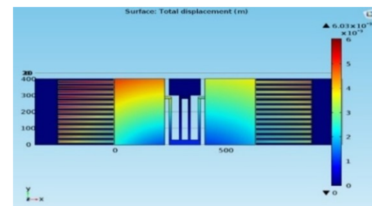

Fig. 5. Total Displacement measurement of the comb.

Simulations on proposed accelerometer is carried out to comprehend the effect of frequency, stress and acceleration on the displacement of the proof mass from the reference when external force is applied on it. From the frequency response of the accelerometer shown in Fig. 8, it is noted that the band width is 1kHz. The stress analysis of the beams shows that the springs are under the maximum pressure at the point where they are connected to the proof mass (see Fig. 8b). As can be seen in Fig. 9, the proof mass's displacement is linear with the change in acceleration.

4.1. Step response of the proposed system

In this system, output voltage is used for the measurement analysis of the device after the electrical output signal is interfaced to the analog circuit for capacitance to voltage conversion. The dynamic behavior of the accelerometer is administered by Newton's second law of motion [9].

The value of the damping ratio has a direct impact on the nature of system response (ζ) [10]. The system has

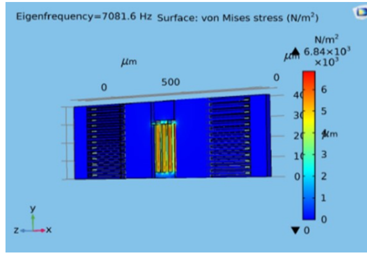

Fig. 6. Stress evaluation in springs.

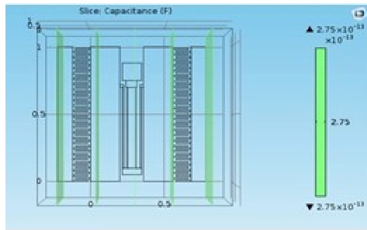

Fig. 7. Capacitance simulation of the structure.

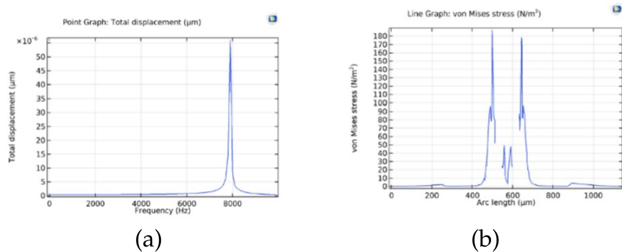

(a) (b)

Fig. 8. (a) Frequency response & (b) Stress analysis

undergone a dynamic study, and its behavior has been analyzed. COMSOL Multiphysics is used to study the dynamic performance of the capacitive accelerometer in Time dependent domain. The simulations were conducted by exerting a lateral force on the proof mass at different damping values. As may be seen in Fig. 10a, the settling time with zero damping is 3 seconds. Fig. 10b shows that when the theoretically calculated value of $\zeta = 0.05$ was used, both the oscillation and the settling time were drastically decreased to 1 second. So, it is understood that the damping value has an impact on the accelerometer response. Further, the behavior of the device was recorded after the damping coefficient value was changed to 0.1, as shown in Fig. 10c.

The system response at $\zeta = 0.5$ is shown in Fig. 10d. Increase in damping resulted in further decrease in oscillations after first overshoot and increase in the displacement value of the proof mass. This increased value of displacement will also dictate the possible maximum output of the accelerometer for the in-plane sensing. Hence it is concluded that the proposed accelerometer is underdamped,

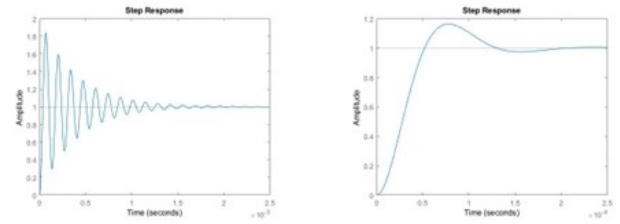

Fig. 9. Displacement analysis

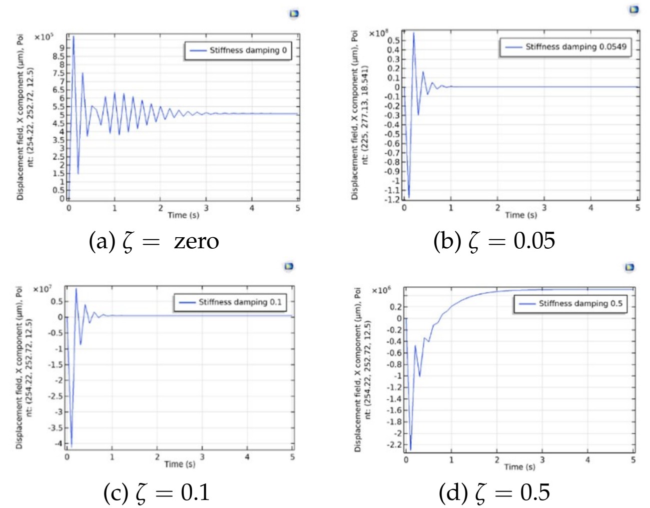

(a) $\zeta =$ zero (b) $\zeta = 0.05$

(c) $\zeta = 0.1$ (d) $\zeta = 0.5$

Fig. 10. Response of accelerometer with different damping values

and the performance can be improved by increasing the ζ value.

5. Fabrication and characterization of the accelerometer

The fabrication of the accelerometer is carried out through the SOIMUMPS process at MEMSCAP foundry. This Process serves as the foundation for the accelerometer design addressed in this work. For high aspect ratio micromachining, a SOI wafer with structural layer thickness of 25μm silicon, 2μm oxide layer and a 400μm base or handle layer is employed. This SOI wafer is dry etched to fabricate the proposed structure. However, the higher comb overlap area caused by the thick structural layer combined with a narrow gap between fingers (achieved using DRIE) results in high capacitance values [11]. It is possible to design and implement longer beams using SOIMUMPs for enhanced sensitivity, but with significantly reduced cross-axis sensitivity and virtually no friction. The cross section of the proposed structure fabricated using SOI MUMPs process is shown in Fig. 11 . The SEM image of the fabricated accelerometer is as shown in Fig. 12.

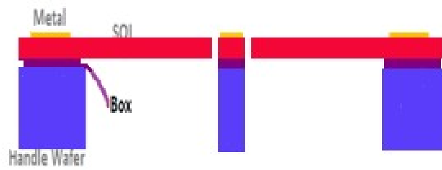

Fig. 11. Cross section of Accelerometer of SOIMUMPS wafer.

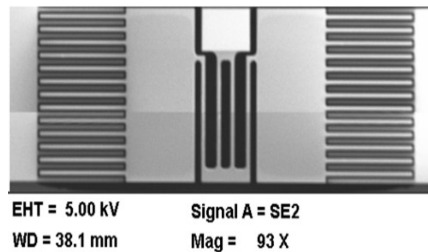

Fig. 12. SEM image of accelerometer .

To verify the performance of the fabricated accelerometer, the characterization of the device is carried out at Micro and Nano Characterization Facility (MNCF) at Centre for Nano Science and Engineering (CeNSE), IISc, Bangalore. The accelerometer is tested at probe station (Agilent 4294A) and is observed that, the device actuated when a voltage of 10V was applied to the electrodes as shown in the Fig 13.a. The frequency is measured from Laser Dopler Vibrometry (LDV- Polytec MSA 500) shown in Fig. 13.b. and it was noted that the first resonant frequency obtained is 10.55kHz as shown in Fig. 13.c.

$C-V$ measurement is carried out at probe station to understand the capacitance-voltage relationship. The capacitance values of C1 and C2 obtained from the test results are found to be 0.36pF and 0.85pF. Fig. 14.a and Fig. 14.b shows the $C-V$ measurement test results for C1 and C2 when a voltage of -10v to $+10$v was applied at 12kHz.

Dynamic study on the fabricated device was carried out using Laser dopler vibrometer and the transient analysis was performed. Fig. 15 is the screenshot of the device which indicates the position where the transient analysis is being conducted and Fig. 16 shows the displacement vs time plot. Also, a test was performed to obtain frequency response and the bode diagram was plotted as displayed in Fig. 17.

6. Results and discussion

The SOI MEMS capacitive single axis accelerometer is designed and simulated using COMSOL Multiphysics and fabricated using SOIMUMPs process. Characterization of the device is done to understand the frequency response

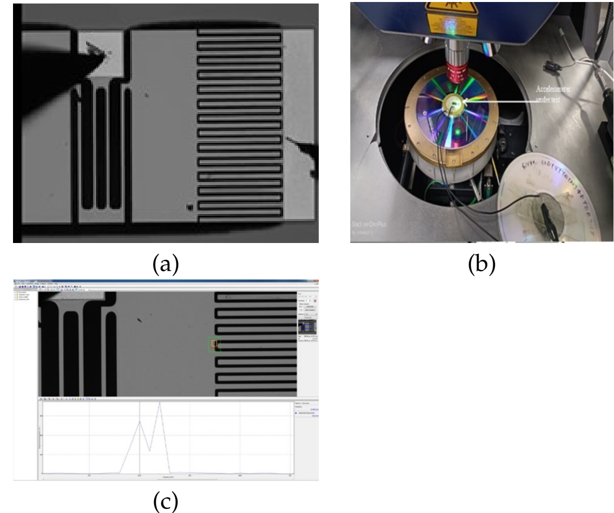

(a) (b) (c)

Fig. 13. (a) Accelerometer at probe station & (b) Device under test (LDV) & (c) Frequency response from LDV

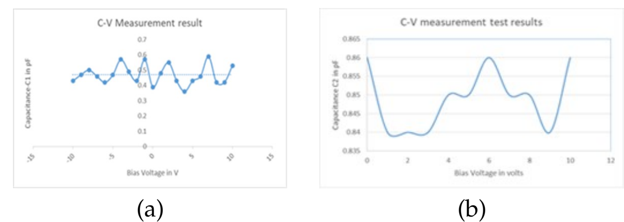

(a) (b)

Fig. 14. (a) C-V measurement for C1 & (b) C-V measurement for C2

and the capacitance is measured on either side of the proof mass. Table 2 gives the comparison of the analytical and simulated values of the performance parameters of the accelerometer. It is observed that the simulated values are in the near range of the calculated values.

The frequency of the fabricated device measured from LDV is 10.5kHz whereas the simulated value of the accelerometer is 7.41kHz. This mismatch in the frequency is due to the change in the fabrication environment which may not be considered in simulations. From the $C-V$ measurement, the capacitances C1 and C2 are found to be 0.36pF and 0.85pF when 10 V is applied to the electrodes whereas the differential capacitance obtained from the simulation is 0.298pF. This difference in the capacitance is due to the fabrication process error, parasitic capacitance and the residual stress which is neglected while performing the simulations and analytical calculation.

However, this offset shall be taken care of while measuring the acceleration. In addition, as can be seen in Fig. 18a and Fig. 18b, the image of the accelerometer captured from the optical profilometer; the proof mass of the accelerom-

Table 2. Comparison of the performance parameters of the accelerometer.

Performance Parameter	Analytical value	Simulated value
Natural frequency	7.41kHz	7.07kHz
Static capacitance	0.28199pF	0.298pF
Displacement sensitivity	$4.5096^{*}10^{-9}$ m/g	$6.03*10^{-9}$ m/g

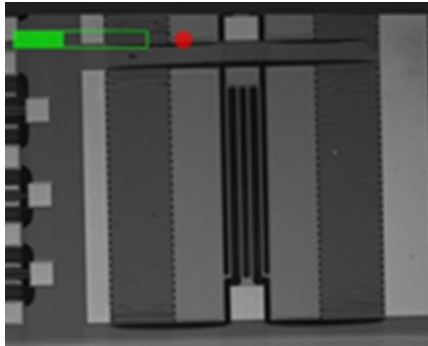

Fig. 15. Transient analysis on the device

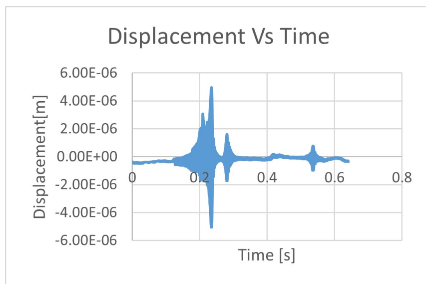

Fig. 16. Displacement of the sensing comb with time

eter is not uniformly suspended on the springs due to its huge size. It can be observed that the proof mass is bulking and therefore the capacitance on either side (C1 and C2) cannot be the same and hence the differential capacitance of the fabricated device is different from the simulated one.

Since this design exhibits a linear force-displacement characteristic, an electrostatic spring constant cannot be formed. Additionally, it exhibits a very low sensitivity because it uses variable overlap area topology. This arrangement is typically employed in the actuating parts of the sensor due to its properties like linearity and low

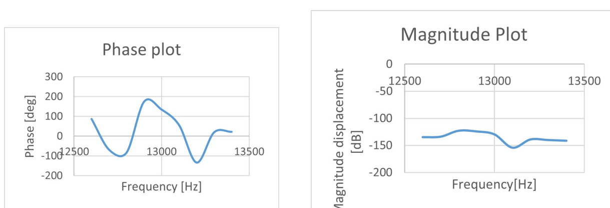

Fig. 17. Magnitude and Phase plot of the fabricated device

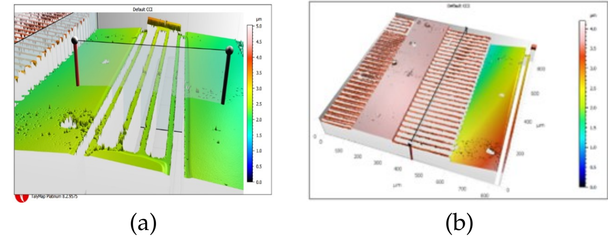

(a) (b)

Fig. 18. (a) Bulking of proof mass (top view) & (b) Bulking of proof mass (front view)

sensitivity.

7. Conclusion

MEMS accelerometers are inertial sensing devices that meet the demands of numerous applications for high performance, low power, integrated functionality, and small size. In this study, an effort is made to thoroughly design, model and perform sensitivity analysis and simulation of a single axis MEMS-based capacitive accelerometer. The results of the COMSOL simulations are nearly identical to the calculated analytical values. The key problem with these simulations is that the capacitance is essentially constant with varying acceleration, so a change in output voltage cannot be predicted using the two capacitances C1 and C2 in differential mode as obtained from the C-V measurement of the fabricated accelerometer. The proposed device is found to resonate at a frequency of 10.5 kHz, which is appropriate for condition-based monitoring applications. With application-specific functionality, thorough factory calibration that reduces costs and production test time, and a straightforward programmable interface that ensures highly precise integration that is simple to implement, intelligent sensor accelerometers offer further integration and improved performance.

Acknowledgement

This work is a part of ISSS community chip activity supported by Institute for Smart Structures and Systems (ISSS), IISc, Bangalore. To complete this work, the authors warmly acknowledge the support provided by Prof. Ananth Suresh, Professor, IISc Bangalore and Dr. Sudhanshu, Founder & CTO at INFAB Technologies, Bangalore. The authors

thank the Department of Electrical and Electronics Engineering, Center for Nano materials and MEMS, NMIT and authorities of Nitte Meenakshi Institute of Technology, Bangalore for their continuous support and encouragement. The authors extend their sincere gratitude to Visveswaraya Institute of Technology, Belagavi for the opportunity and support.

References

[1] V. Baban, D. Argintaru, and E. Constantinescu. "Analysis and simulation of a MEMS based accelerometer used to monitor the movement of a sea waves". In: *Advanced Topics in Optoelectronics, Microelectronics, and Nanotechnologies XI*. ***12493***. SPIE. 2023, 509–515. DOI: 10.1117/12.2643251.

[2] M. Preeti, K. Guha, K. L. Baishnab, A. Sastry, K. Dusarlapudi, and K. N. Raju, (2022) *"Analysis of a proof mass structure of a capacitive accelerometer as wearable sensor for health monitoring"* **Micro and Nanoelectronics Devices, Circuits and Systems: Select Proceedings of MNDCS 2021**: 315–327. DOI: 10.1007/978-981-16-3767-4_30.

[3] R. Mukhiya, P. Agarwal, S. Badjatya, M. Garg, P. Gaikwad, S. Sinha, A. Singh, and R. Gopal, (2019) *"Design, modelling and system level simulations of DRIE-based MEMS differential capacitive accelerometer"* **Microsystem technologies *25***: 3521–3532. DOI: 10.1007/s00542-018-04292-0.

[4] M. Manvi and K. M. Swamy, (2022) *"Microelectronic materials, microfabrication processes, micromechanical structural configuration based stiffness evaluation in MEMS: A review"* **Microelectronic Engineering**: 111854. DOI: 10.1016/j.mee.2022.111854.

[5] J. Huang, Y. Zhao, G. M. Xia, Q. Shi, and A. P. Qiu, (2022) *"Systematic modeling of a MEMS resonant accelerometer based on displacement coordination"* **IEEE Sensors Journal *22***(7): 6454–6465. DOI: 10.1109/JSEN.2022.3155605.

[6] S. Veena, A. Sthuti, H. Suresh, M. Nagaraj, et al., (2022) *"Simulation and analysis of suspension based single axis mems capacitive accelerometer"* **International Journal of Basic and Applied Science *11***(3): 107–116. DOI: 10.35335/ijobas.v11i3.119.

[7] N. Rai, H. Suresh, V. S. Nagaraja, et al., (2021) *"Design, modelling, and simulation analysis of a single axis MEMS-based capacitive accelerometer"* **arXiv preprint arXiv:2111.03816**: DOI: 10.14445/22315381/IJETT-V69I10P211.

[8] C. Likhith, K. Asha, and N. Krishnaswamy. "Design and Simulation of Parallel Plate-Comb Type Mems Capacitive Accelerometer Using COMSOL". In: *Micro and Nanoelectronics Devices, Circuits and Systems: Select Proceedings of MNDCS 2022*. Springer, 2022, 389–405. DOI: 10.1007/978-981-19-2308-1_40.

[9] S. Veena, N. Rai, A. M. R. Morey, H. Suresh, and H. Shaik. "Design and Simulation of MEMS Based Capacitive Accelerometer". In: *IoT and Analytics for Sensor Networks: Proceedings of ICWSNUCA 2021*. Springer. 2022, 207–223. DOI: 10.1007/978-981-16-2919-8.

[10] K. Shibata, A. Uchiyama, A. Onishi, K. Machida, P. Chakraborty, S.-I. Iida, T. Konishi, M. Sone, Y. Miyake, and H. Ito, (2022) *"Simplified Analytical Damping Constant Model for Design of MEMS Capacitive Accelerometer With Gold Perforated Proof-Mass Structure"* **IEEE Sensors Journal *22***(15): 14769–14778. DOI: 10.1109/JSEN.2022.3184340.

[11] M. K. Dounkal, R. Bhan, and N. Kumar, (2020) *"A new improved vertical comb type differential capacitive sensing micro accelerometer using silicon-on-insulator wafer technology"* **Journal of Micromechanics and Microengineering *30***(10): 105008. DOI: 10.1088/1361-6439/ab9b13.